# Lipid and Signal Peptide-Induced Conformational Changes within the C-Domain of Escherichia coli SecA Protein

**ARTICLE** *in* BIOCHEMISTRY · MARCH 2001

Impact Factor: 3.02 · DOI: 10.1021/bi002058w · Source: PubMed



**3 AUTHORS**, INCLUDING:

Donald Oliver
Wesleyan University
**84** PUBLICATIONS **5,126** CITATIONS

SEE PROFILE

# Lipid and Signal Peptide-Induced Conformational Changes within the C-Domain of *Escherichia coli* SecA Protein

Haiyuan Ding, Ishita Mukerji, and Donald Oliver*

*Department of Molecular Biology and Biochemistry, Wesleyan University, Middletown, Connecticut 06459, USA*

*Received August 31, 2000; Revised Manuscript Received November 29, 2000*

ABSTRACT: SecA ATPase is an essential component of the Sec-dependent protein translocation machinery. Upon interaction with the plasma membrane containing SecYE, preprotein, and ATP, SecA undergoes cycles of membrane insertion and retraction resulting in the translocation of segments of the preprotein to the trans side of the membrane. To study the structural basis of SecA function, we employed fluorescence spectroscopy along with collisional quenchers with a set of SecA proteins containing single tryptophan substitutions. Our data show that among the seven naturally occurring tryptophan residues of *Escherichia coli* SecA, only the three tryptophan residues contained within the C-domain contributed significantly to the fluorescence signal, and they occupied distinct local environments in solution: Trp723 and Trp775 were found to be relatively solvent accessible and inaccessible, respectively, while Trp701 displayed an intermediate level of solvent exposure. Exposure to increased temperature or interaction with model membranes or signal peptide elicited a similar conformational response from SecA based upon the fluorescence signals of the SecA-W775F and SecA-W723F mutant proteins. Specifically, Trp775 became more solvent exposed, while Trp723 became less solvent accessible under these conditions, indicating similarities in the overall conformational change of the C-domain promoted by temperature or translocation ligands. Only Trp701 did not respond in parallel to the different conditions, since its solvent accessibility changed only in the presence of signal peptide. These results provide the first detailed structural information about the C-domain of SecA and its response to translocation ligands, and they provide insight into the conformational changes within SecA that drive protein translocation.

During the past two decades, considerable attention has been focused on the steps that lead to the specific targeting and translocation of proteins across biological membranes. The relative simplicity and tractability of *Escherichia coli* make it an ideal system in which to study this process. Genetic and biochemical methods have allowed the identification and characterization of the major Sec-dependent pathway that is responsible for the biogenesis of most secretory and many integral membrane proteins (*1*, *2*). This system consists of the cytosolic SecB chaperone, the SecA translocation ATPase, SecYE protein that makes up the translocation channel, and integral membrane accessory proteins SecG and SecDF. Both SecB-dependent and independent proteins are delivered to SecA, which has binding sites for SecB and preprotein as well as SecYE (*3*−*5*). Upon binding of preprotein and ATP, SecA undergoes a major conformational change that allows it to insert into the translocation channel (*6*−*8*). ATP hydrolysis and preprotein release promote SecA deinsertion and set the stage for additional rounds of SecA membrane cycling that facilitates the stepwise translocation of preproteins (*9*). SecG is a small integral membrane protein that facilitates SecA membrane cycling by undergoing a topology inversion that is coupled to the cycle of SecA insertion and retraction (*10*). SecDF stabilizes the membrane-inserted form of SecA and appears to prevent preprotein backsliding by slowing the movement of the translocating polypeptide chain (*11*).

SecA makes a number of interactions with critical components of the translocation machinery. These include ATP, preprotein, SecB, SecY, SecG, and anionic phospholipids (*4*−*6*, *12*−*17*). SecA consists of two structural domains of 65 kDa (N-domain) and 30 kDa (C-domain) (*18*). Located in the N-domain are two nucleotide-binding domains, NBD-I and NBD-II, that flank the proposed preprotein-binding region (*12*, *19*). The C-domain contains a region for binding SecB and phospholipids that is located in a cysteine-rich region at the C-terminus (*5*, *16*). The N-domain also contains the SecYE-specific binding activity of SecA, while the C-domain binds to membranes nonspecifically through partitioning into phospholipids (*20*). During protein translocation both the N- and C-domains have been reported to undergo membrane cycling, where the preprotein-binding and C-terminal regions become periplasmically exposed upon SecA membrane insertion (*8*, *21*, *22*).

Elucidation of SecA conformational cycling and its regulation by the various translocation components is critical to understand the protein translocation cycle. Previous studies have identified at least two distinct conformational states of SecA: a compact form that is favored at low temperature or upon ADP binding and a more extended or relaxed conformation that is favored at high temperature or upon binding adenylyl-imidodiphosphate (AMP-PNP), preproteins, or model membranes containing anionic phospholipids (*6*,

* Corresponding author: Phone: 860-685-3556; fax: 860-685-2141; e-mail: doliver@wesleyan.edu.

10.1021/bi002058w CCC: $20.00 
Published on Web 01/18/2001

*15*, *23*). This latter state presumably corresponds to a transitional form of SecA that bears similarities to the membrane-inserted form of the protein. The change in SecA conformation has been followed previously utilizing intrinsic Trp fluorescence and corresponds to SecA's endothermic transition (*15*). Recent work indicates that SecA proteins that confer azide-resistant (*azi*) or signal sequence suppressor (*prlD*) phenotypes are shifted in their endothermic transition toward the relaxed state, and they display a reduced affinity for ADP and a higher nucleotide exchange rate (*24*). These observations are consistent with the ability of the respective strains to escape azide inhibition or suppress signal sequence defects.

A determination of the crystal structure of SecA protein is currently in progress (J. Hunt, S. Weinhauf, D. Oliver, and J. Deisenhofer, manuscript in preparation). This approach, however, will not shed light on the various local or global structural fluctuations that occur during the SecA-dependent protein translocation cycle. By contrast, spectroscopic techniques involving fluorescence emission and collisional quenching of emission by solutes can provide sensitive probes of the conformational states of proteins and their modulation by ligands. The emission of tryptophan is highly sensitive to its local environment, and therefore, it is often used as a reporter group for changes in protein conformation (*25*, *26*). In previous work, Trp fluorescence has been used successfully to monitor conformational changes of proteins during the protein folding process (*27*, *28*) and the insertion of peptides into membrane systems (*29*). Because of this sensitivity to local environment and structure, we have utilized Trp fluorescence to study the conformational changes of SecA protein.

In this work, a family of SecA proteins containing a single substitution of Trp to Phe for each of the seven Trp residues of SecA protein was constructed. Comparison of the fluorescence properties of this set of proteins under various conditions allowed us to assign the contribution of individual Trp residues to the fluorescence spectra, determine their solvent accessibility, and identify those residues that are responsible for the spectroscopic changes induced by the endothermic transition or by phospholipid or signal peptide binding. Our results provide the first detailed structural information about the C-domain of SecA and its response to temperature or translocation ligands, and they provide a basis for understanding SecA conformational changes during the protein translocation cycle.

## EXPERIMENTAL PROCEDURES

*Materials*. DOPC[1] and DOPG were purchased from Avanti Polar Lipids (Pelham, AL). Acrylamide and most common chemicals were obtained from Sigma. The LamB signal peptides were kindly provided by Lila Gierasch (U. Mass.).

*Mutagenesis and Complementation*. TGG (Trp) to TTC (Phe) substitutions were introduced into the *secA* gene contained on pT7 secA2 (*12*) utilizing appropriate oligonucleotide primers and a QuikChange site-directed mutagenesis kit (Stratagene) as described by the manufacturer. All mutations were confirmed by DNA sequence analysis. Plasmids were transformed into BL21.19 ($\lambda$DE3) [*secA13-(Am) supF(Ts) trp(Am) zch::Tn10 recA::CAT clpA::KAN*] (*12*) and checked for *secA* complementation by growth and single colony formation at 42 °C as described previously (*12*).

*Purification of Mutant SecA Proteins and ATPase Assays*. SecA proteins were overproduced from BL21.19 containing the appropriate plasmid and purified by affinity chromatography on Cibacron Blue agarose (Sigma) as described previously (*12*). Protein concentration was determined using the Bradford assay (BioRad) with bovine serum albumin as a standard. SecA ATPase activities were determined by the Malachite green method (*30*) utilizing the modifications described in Mitchell and Oliver (*12*). ATPase activity was calculated using the following formulas: endogenous ATPase activity = ATPase activity in the presence of SecA − ATPase activity in the absence of SecA; membrane ATPase activity = ATPase activity in the presence of SecA and IMV − (ATPase activity in the presence of IMV + endogenous ATPase activity); translocation ATPase activity = ATPase activity in the presence of SecA, IMV, and preprotein − membrane ATPase activity. SecA-depleted IMV and the chimeric preprotein comprised of the *E. coli* alkaline phosphatase signal sequence and *Staphylococcal* nuclease with K97C and W140H substitutions were prepared as described by Kim et al. (*31*) and Cabelli (*32*), respectively.

*Fluorescence Measurements*. Steady-state fluorescence spectra were recorded at 20−30 $\mu$g/mL SecA protein in TKE buffer (25 mM Tris-HCl, pH 7.5, 25 mM KCl, 1 mM EDTA) on a FluoroMax-2 spectrofluorometer (Instruments S. A., Metuchen, NJ) with a Neslab programmable water bath with a remote sensor. Sample was placed in a quartz cuvette with a 1-cm excitation and 0.4-cm emission path length. The excitation and emission slits were set at 0.71 mm to give a 3-nm band-pass. Spectra were scanned at a rate of 1 nm/s from 320 to 450 nm using an excitation wavelength of 297 nm. Two or more data sets were collected for all experiments, and they gave rise to essentially identical results in all cases. Light scattering due to the presence of LUV was assessed by comparing the fluorescence spectra of *N*-acetyl-L-tryptophanamide, LUV, and *N*-acetyltryptophamide plus LUV or SecA, LUV, and SecA plus LUV in the range of 300−450 nm using an excitation wavelength of 297 nm.

*Preparation of LUV*. Synthetic phospholipids dissolved in chloroform were dried under a stream of nitrogen and dried further under high vacuum for at least 1 h. Lipids were resuspended thoroughly in TKE buffer and subjected to five freeze−thaw cycles. LUV were made by passing samples 20 times through polycarbonate filters (pore diameter 100 nm) using an extrusion apparatus, LiposoFast-Basic (Avestin, Ottawa, Canada). For binding studies the LUV stock solution was 10 mg/mL DOPC/DOPG (1:1, w/w).

*Acrylamide Quenching Experiments*. A 4 M acrylamide stock solution was prepared in TKE buffer. Quenching experiments were carried out by adding aliquots of the acrylamide stock solution or TKE buffer to the test solution. The results obtained with TKE buffer were used to correct for the effect of dilution on the experimental values.

[1] Abbreviations: AMP-PNP, adenylyl imidodiphophate; DOPC, L-$\alpha$-1,2-dioleoylphosphatidyl-choline; DOPG, 1,2-dioleoylphosphatidyl-glycerol; IMV, inverted membrane vesicles; LamB-KRR, LamB signal peptide with Lys Arg Lys inserted between the sixth and seventh residue; LamB-KRR19C$\Delta$78, similar to LamB-KRR but also missing residues 10−13 along with a Cys substitution at residue 19 of LamB; LUV, large unilamellar vesicles; NBD-I or NBD-II, high or low affinity nucleotide-binding domain, respectively.

*Data Processing*. All fluorescence emission spectra were recorded utilizing Datamax (Galactic Industries Corp.). Values of fluorescence intensity at specific emission wavelengths were taken and processed utilizing Prism 2.0 software (GraphPad Software, Inc.). For quenching experiments, data points were averaged from two sets of experiments, and the Stern−Volmer equation $F_0/F = 1 + K_{SV}[Q]$ was used for curve fitting. For determination of the affinity of SecA for LUV, the following equation that is based on the assumption of a single binding-site was used for curve fitting: $\Delta F/F_0 = \Delta F_{max}/F_0[LUV]/(K_d + [LUV])$, where $F$ and $F_0$ are the fluorescence intensities in the presence and absence of LUV, respectively, $\Delta F$ is the difference between $F$ and $F_0$, and $\Delta F_{max}$ represents the maximal difference in fluorescence intensity. The values of $\Delta F_{max}$ and $K_d$ were extracted from curve fitting. For experiments measuring the endothermic transition or peak shift of SecA protein with increasing temperature, the data was fitted to a sigmoidal curve by employing the following equation: $Y = Y_{initial} + (Y_{final} - Y_{initial})(1 + 10^{(Tm - X)/k})$, where $Y$ represents $F/F_0$ or $F_{330}/F_{355}$, $X$ represents temperature, $T_m$ is the midpoint of the curve, and $Y_{final}$ and $Y_{initial}$ are the values for $Y$ at final and initial temperatures, respectively.

## RESULTS

*Characterization of SecA Proteins Containing Single Trp to Phe Substitutions*. *E. coli* SecA protein contains seven Trp residues at positions 349, 519, 541, 622, 701, 723, and 775 (*33*). According to previous reports Trp349 is located within the putative preprotein-binding region, Trp519 and Trp541 are located within NBD-II, Trp622 is located at the junction of NBD-II and the C-domain, and Trp701, Trp723, and Trp775 are located within the C-domain of SecA (*12*, *18*, *19*). To assess the contributions of individual Trp residues to SecA fluorescence we employed site-directed mutagenesis to produce a set of seven SecA proteins each containing a single Trp to Phe substitution. While this approach has the disadvantage that each protein still contains six Trp residues, complicating the interpretation of the fluorescence data, it has the advantage of minimally altering the sequence and properties of a given SecA protein. We found, for example, that certain combinations of multiple Trp substitutions altered the biochemical properties of SecA protein rendering it membrane associated and difficult to purify (Ding, Mukerji, and Oliver, unpublished results). These observations suggest that more extensive substitutions within SecA are likely to alter its normal conformational equilibrium and its response to various translocation ligands.

The seven Trp substitution mutants were engineered into pT7 secA2, which expresses *secA* under a T7 promoter. BL21.19 was used as the host for these plasmids, since it contains the *secA13(Am) supF(Ts)* alleles that allow for the conditional expression of chromosomal *secA*. Each Trp substitution mutant was named according to the position of the substitution [e.g., BL21.19 (pT7 secA-W349F)]. The biological function of each *secA* allele was tested by complementation (see Experimental Procedures). All seven mutants were able to grow normally both with respect to the size and efficiency of colony formation under conditions where the mutant SecA protein was expressed at chromosomal levels and was the only source of SecA within the cell (M63 minimal glucose plates at 42 °C) (data not shown). This result suggests that the *in vivo* activity of these mutant SecA proteins is similar to wildtype SecA.

SecA protein from each strain was overproduced and purified. Analysis of the purified proteins by SDS−PAGE and staining with Coomassie brilliant blue revealed a single species of the predicted molecular mass with greater than 95% purity (data not shown**)**. SecA protein has been shown previously to possess three distinct ATPase activities: an endogenous ATPase activity that is stimulated by binding IMV (membrane ATPase) or IMV and preprotein (translocation ATPase) (*34*). ATPase assays of the mutant proteins indicated that they possessed comparable endogenous, membrane, and translocation ATPase activities to those of wildtype SecA protein (data not shown). We conclude that our seven mutant SecA proteins were normally active both *in vivo* and *in vitro*, and therefore they should yield valuable information regarding SecA structure−function relationships in our spectroscopic assays.

*Contribution of Each Trp Residue to SecA Fluorescence*. Construction of the Trp substitution mutants allowed us to determine the contribution of each Trp residue to the overall fluorescence spectrum of SecA protein. We used an excitation wavelength of 297 nm in this study since the other two naturally occurring aromatic amino acids, Phe and Tyr, have little absorption at this wavelength and therefore do not contribute to the fluorescence spectrum, and energy transfer between identical tryptophyl groups is decreased significantly or undetectable by excitation at the red edge of the absorption spectrum (*35*). Examination of the fluorescence spectra of SecA proteins showed that the fluorescence intensity of wildtype SecA, SecA-W349F, SecA-W519F, SecA-W541F, and SecA-W622F was essentially identical (Figure 1, panel A), while that of SecA-W701F, SecA-W723F, and SecA-W775F was decreased significantly (Figure 1, panel B). This result suggests that Trp701, Trp723, and Trp775 are the major contributors to SecA fluorescence under these conditions. Since the apparent lack of contribution of Trp349, Trp519, Trp541, and Trp622 to the overall fluorescence of SecA protein was unexpected, we critically tested this result by examining the fluorescence of a SecA protein lacking Trp701, Trp723, and Trp775, SecA-W701F/W723F/W775F. We found that this protein, which was biologically active *in vivo* based on our complementation assay, was only weakly fluorescent (Figure 1, panel B). Figure 2, panel A shows the fluorescence spectra of the different SecA proteins corrected for their absorbance at 297 nm. The increase in relative fluorescence yield of SecA-W349F, SecA-W519F, SecA-W541F, and SecA-W622F suggests that these Trp residues contributed strongly to the absorbance at 297 nm, but they did not contribute significantly to the overall emission. Furthermore, the increase in relative quantum yield and the similarity in emission profile with respect to wildtype SecA are also suggestive that energy transfer to other Trp residues is not a significant source of fluorescence quenching for these residues. By contrast, the relative fluorescence yield of SecA-W701F, SecA-W723F, and SecA-W775F was significantly decreased as compared to wildtype SecA, indicating that Trp701, Trp723, and Trp775 are the major contributors to the fluorescence emission under these conditions. Figure 2, panel B shows the difference spectrum for each Trp residue. Only Trp701, Trp723, and Trp775 have positive contributions to the overall quantum yield of SecA

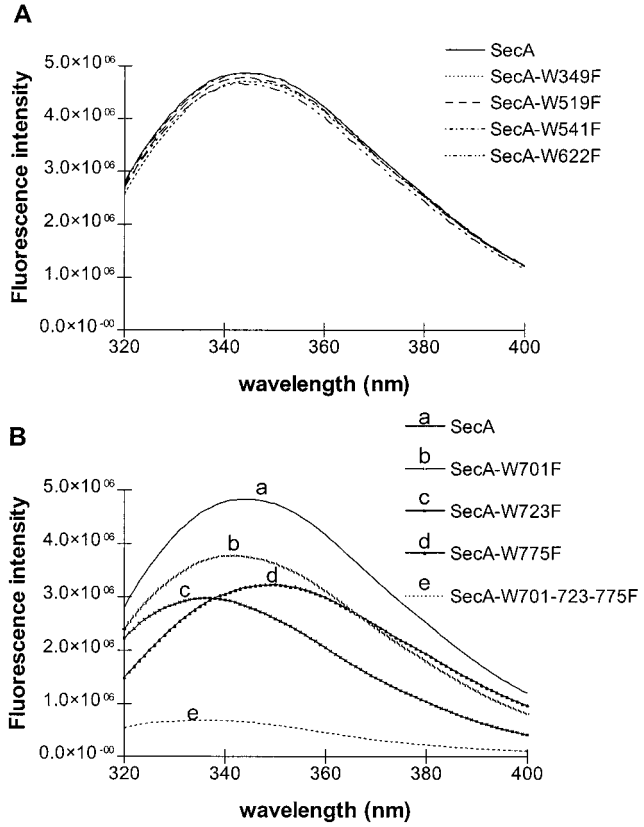


FIGURE 1: Fluorescence spectra of wildtype and mutant SecA proteins: (A) wildtype SecA and four N-domain Trp substitution SecA proteins (SecA-W349F, SecA-W519F, SecA-W541F, and SecA-W622F); (B) wildtype SecA, three C-domain Trp substitution SecA proteins (SecA-W701F, SecA-W723F, and SecA-W775F) and SecA-W701F/W723F/W775F. Fluorescence spectra of 0.15 $\mu$M SecA in TKE buffer were recorded at 24 °C with excitation at 297 nm.

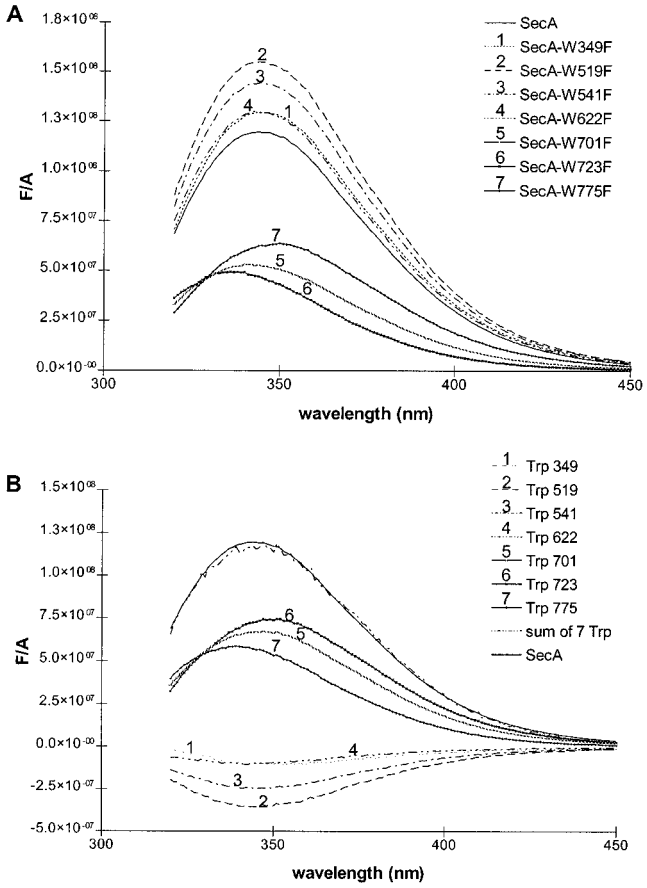


FIGURE 2: Contribution of individual Trp residues to SecA fluorescence. Fluorescence spectra of 0.15 $\mu$M SecA in TKE buffer were recorded at 24 °C with excitation at 297 nm. (A) Absorbance corrected spectrum of indicated SecA protein; (B) spectrum of individual Trp residues derived by subtraction of the mutant protein fluorescence spectrum from that of wildtype SecA. A comparison of the sum of the difference spectra for the individual Trp residues to that of wildtype SecA is given also.

protein, where Trp723 contributes most, followed in order by Trp701 and Trp775. Since these three Trp residues are contained solely within the C-domain of SecA, our results indicate that fluorescence studies of SecA provide a specific measure of events that occur within this region of the protein. We note further that the sum of the relative fluorescence quantum yield of the seven Trp residues is almost identical to that of wildtype SecA (Figure 2, panel B). This result indicates that the single amino acid substitutions were unlikely to cause a major conformational change in these proteins and that energy transfer between Trp residues within SecA was a relatively minor contribution to the overall fluorescence spectrum. We also measured the contribution of each Trp residue to the overall SecA fluorescence intensity in the presence of several SecA ligands, such as signal peptide, ADP, and phospholipid. The results were also consistent with the above observations (data not shown), indicating that Trp701, Trp723, and Trp775 were still the major contributors of SecA fluorescence emission under these conditions.

*Local Environment of Trp701, Trp723, and Trp775*. Since the amplitude and wavelength of Trp fluorescence emission are dependent on the polarity of the local environment and the mobility of Trp residues, the fluorescence emission maxima ($\lambda_{max}$) often provide valuable information about the solvent accessibility of Trp residues within a protein. Trp723 and Trp701 had $\lambda_{max}$ values of 354 and 347 nm, respectively (Figure 2, panel B), indicating that they are relatively solvent exposed in SecA in its solution state. By contrast, Trp775 appears to be a buried residue based on its $\lambda_{max}$ of 335 nm. This result is consistent with that of den Blaauwen *et al.* (*23*), who studied the fluorescence properties of SecA proteins engineered to contain solely Trp701 or Trp775.

To confirm these inferences, we directly assessed Trp solvent accessibility utilizing acrylamide as a fluorescence quencher. Acrylamide is a collisional quencher (*36*), in which the amount of quenching is linearly related to acrylamide concentration as described by the Stern−Volmer equation, $F_0/F = 1 + K_{SV}$ [Q], where [Q] is the quencher concentration and $K_{SV}$ is the Stern−Volmer quenching constant. $K_{SV}$ is the product of $k_q$, the collisional quenching constant, and $\tau_0$, the excited-state lifetime in the absence of quencher. In the experiments that follow we assume that differences in $K_{SV}$ are most likely due to differences in $k_q$, although it remains conceivable but much less likely that $\tau_0$ was altered. Figure 3 is a plot of $F_0/F$ versus acrylamide concentration for the different SecA proteins, where the slope of each curve provides the value of $K_{SV}$ for each protein. SecA-W775F had the highest $K_{SV}$ value and consequently, greatest overall solvent exposure, followed in order by wildtype SecA, SecA-W701F, and SecA-W723F (Table 1). Since the Trp775 to Phe substitution increased the overall solvent exposure of

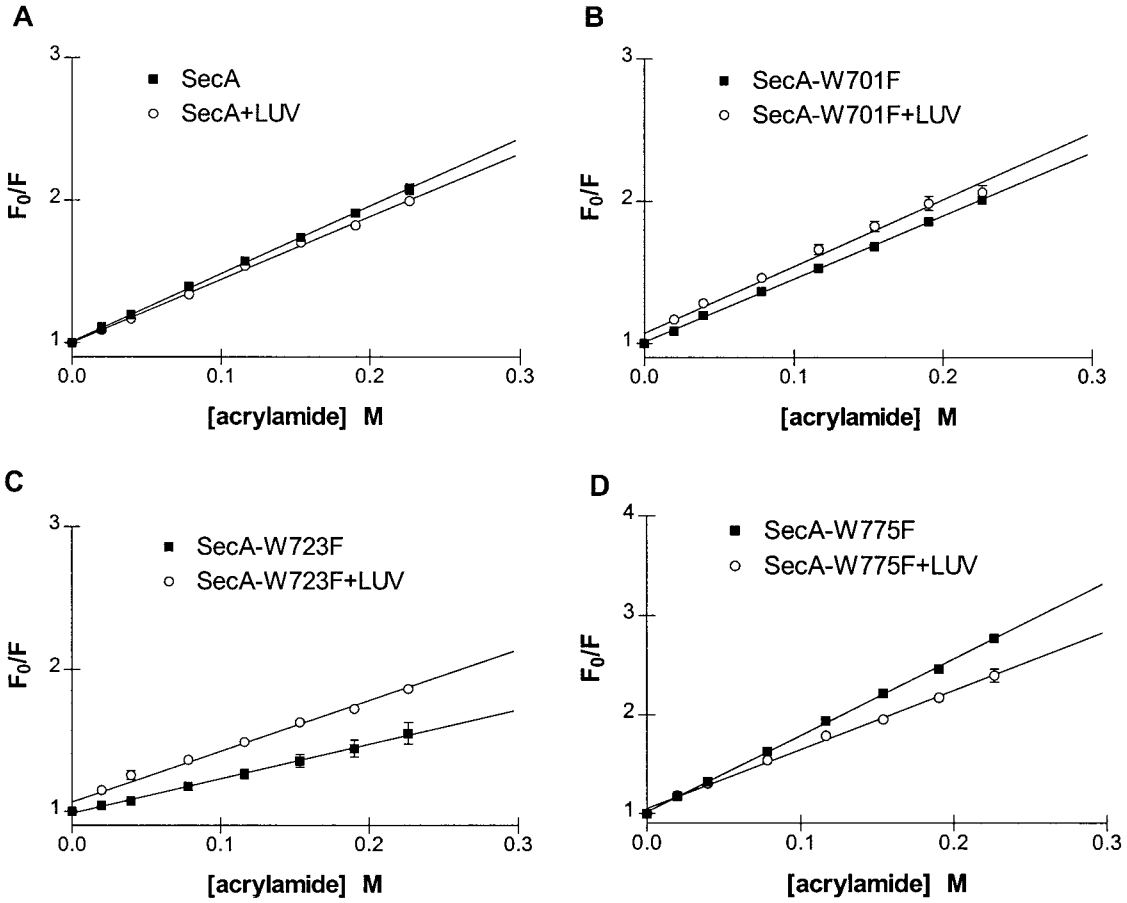


FIGURE 3: Stern−Volmer plots using acrylamide as the quencher for SecA proteins in the absence and presence of LUV. (A) Wildtype SecA, (B) SecA-W701F, (C) SecA-W723F, and (D) SecA-W775F. For experiments with LUV, SecA (25 $\mu$g/mL) proteins were incubated with 300 $\mu$g/mL LUV in TKE buffer for 30 min prior to initiating the experiment. Fluorescence quenching experiments were conducted at 24 °C using 297 nm as the excitation wavelength and 340 nm as the emission wavelength. $F_0$ and $F$ are the fluorescence intensities in the absence and presence of acrylamide, respectively. Values were corrected for dilution. Some error bars are within the range occupied by the symbols.

Table 1: Acrylamide Quenching Constants of SecA Proteins

| | $K_{SV}$ ($M^{-1}$) | | | |
|---|---|---|---|---|
| | SecA | SecA-W701F | SecA-W723F | SecA-W775F |
| protein alone | 4.74 ± 0.04 | 4.44 ± 0.05 | 2.42 ± 0.04 | 7.61 ± 0.08 |
| +LUV | 4.41 ± 0.07 | 4.70 ± 0.22 | 3.56 ± 0.16 | 5.97 ± 0.14 |
| +LamB-KRR | 3.77 ± 0.03 | 2.80 ± 0.02 | 2.47 ± 0.03 | 1.66 ± 0.07 |
| +LamB-KRR19CΔ78 | 5.00 ± 0.03 | 4.65 ± 0.03 | 2.86 ± 0.06 | 8.24 ± 0.10 |

SecA the most, it follows that Trp775 is the most buried Trp residue within the C-domain of SecA. A similar logic indicates that Trp723 is the most solvent exposed Trp residue within the C-domain, while Trp701 displayed an intermediate level of solvent exposure. Our results are in basic agreement with those of Song and Kim (*37*), who obtained a value of 75% exposure for the Trp residues of SecA by comparing iodide quenching for native and denatured SecA protein.

*Environmental Changes of Trp701, 723, and 775 during SecA Interaction with LUV*. The interaction of SecA with the plasma membrane requires both SecYE protein and acidic phospholipids (*3*, *38*, *39*). It has been shown previously that SecA can spontaneously insert into model membranes containing anionic phospholipids (*15*, *40*). Although this insertion is distinct from that which occurs at SecYE after preprotein and ATP binding, it may represent an important model subreaction in the overall protein translocation cycle. In this regard, we have recently shown that when SecA initially binds to IMV, the N-domain is responsible for interaction with SecYE, while the C-domain interacts with phospholipids (*20*). To learn more about the conformational response of the C-domain during its interaction with phospholipids, we first measured the affinity of SecA protein for LUV. Figure 4 shows that the different SecA proteins showed similar affinities for LUV, although the affinity of wildtype SecA was modestly higher than the three mutant SecA proteins. Previously, we have shown that SecA has a $K_d$ between 50 and 70 $\mu$g/mL for small unilamellar vesicles (SUV) with a similar phospholipid composition (*15*). The high degree of curvature of SUV may contribute to a higher affinity for SecA binding than LUV. Figure 3 compares the acrylamide quenching of SecA fluorescence in the presence or absence of saturating levels of LUV. Only a minor difference between these two conditions was noted for wildtype SecA and SecA-W701F, while more striking differences were revealed with the remaining two mutant proteins. Acrylamide quenched the fluorescence of SecA-W723F more strongly in the presence of LUV than in their absence, while the opposite result was observed for SecA-W775F. Light scattering due to the presence of LUV was ruled out as a cause for any differences detected (data not shown). Since the Trp723 to Phe substitution increased the overall exposure of SecA-W723F after LUV addition, it

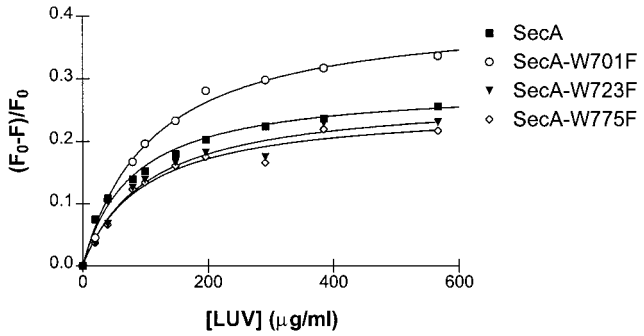


| | Kd (μg/ml) |
|---|---|
| SecA | 78.7 ± 7.7 |
| SecA-W701F | 110.4 ± 8.1 |
| SecA-W723F | 103.6 ± 16.9 |
| SecA-W775F | 96.2 ± 16.9 |

FIGURE 4: Binding of SecA to LUV. SecA protein (0.1 $\mu$M) was incubated with increasing concentrations of LUV in TKE buffer at 24 °C for 30 min prior to initiating the experiment. Fluorescence intensities were measured for sample with ($F$) and without ($F_0$) LUV using an excitation wavelength of 297 nm and emission wavelength of 340 nm.

follows that Trp723 becomes more buried upon SecA lipid binding. A similar logic indicates that Trp775 becomes more solvent exposed when SecA binds to LUV. These results strongly support the hypothesis of Ulbrandt *et al*. (*15*) that SecA undergoes a conformational change upon binding model membranes. These results also indicate that this response minimally involves portions of the C-domain.

*Environmental Changes of Trp701, 723, and 775 during the Endothermic Transition*. We have shown previously that the conformational change of SecA from its more compact to extended state is dependent on temperature as well as phospholipid binding. The fluorescence intensity of SecA decreases sigmoidally as a function of increasing temperature that is characteristic of this conformational transition (*15*). To characterize this conformational change further, we studied the endothermic transitions of our mutant SecA proteins. Plots of $F/F_0$ versus temperature for SecA-W349F, SecA-W519F, SecA-W541F, and SecA-W622F were indistinguishable from that of wildtype SecA both in magnitude and shape (data not shown). This result indicates that the N-domain of SecA does not strongly contribute to the overall fluorescence of either conformational state of SecA, and these mutant SecA proteins have a similar conformational flexibility as wildtype SecA protein. In contrast, similar plots for SecA-W701F, SecA-W723F, and SecA-W775F showed a decreased magnitude as compared to wildtype SecA (Figure 5, panel A). This result indicates that Trp701, Trp723, and Trp775 were the major contributors to the overall fluorescence for both conformational states of SecA. In addition, the midpoint of the endothermic transition ($T_m$) was somewhat reduced for SecA-W723F (38.5 ± 0.8 °C), SecA-W775F (39.0 ± 0.2 °C), and SecA-W701F (39.4 ± 0.3 °C) as compared to wildtype SecA (40.2 ± 0.3 °C), suggesting a modest destabilization of the compact form of SecA as a result of the Trp to Phe substitutions.

Since shifts in fluorescence maxima during the endothermic transition were difficult to visualize from the spectra, we plotted the $F_{330}/F_{355}$ ratio as a function of temperature. This latter method has been shown to more effectively reveal spectral shifts (*41*). Figure 5, panel B shows that during the

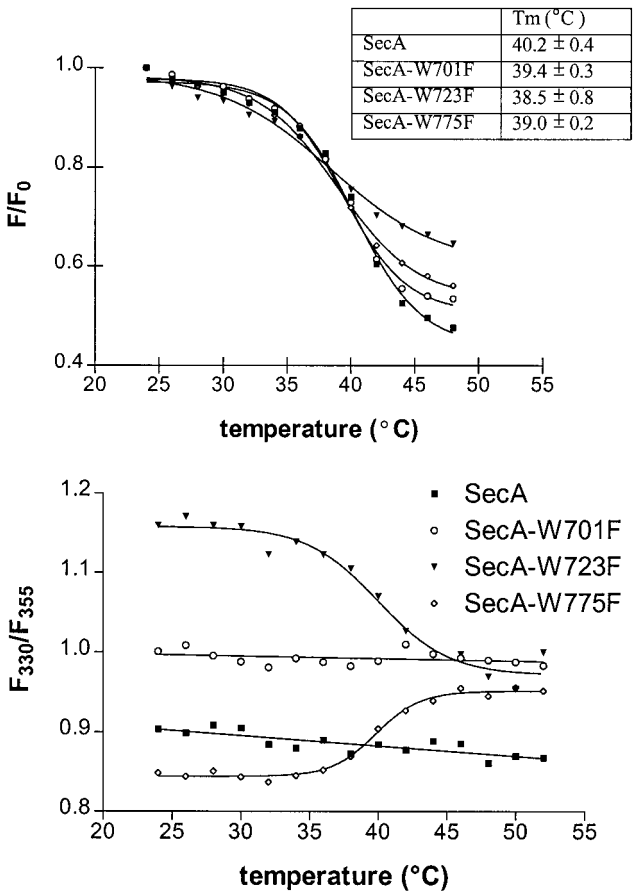


| | Tm (°C) |
|---|---|
| SecA | 40.2 ± 0.4 |
| SecA-W701F | 39.4 ± 0.3 |
| SecA-W723F | 38.5 ± 0.8 |
| SecA-W775F | 39.0 ± 0.2 |

FIGURE 5: Shift in the peak fluorescence of SecA during its endothermic transition. (A) The intrinsic Trp fluorescence intensity at 340 nm relative to that present at the starting temperature ($F/F_0$) of 0.1 $\mu$M of the indicated SecA protein in TKE buffer was measured as a function of temperature at an excitation wavelength of 297 nm. (B) The ratio of emission intensity at 330 and 355 nm ($F_{330}/F_{355}$) as a function of temperature was plotted for the different SecA proteins. Sigmoidal curve fitting was conducted for SecA-W723F and SecA-W775F.

endothermic transition, there was little change in the $F_{330}/F_{355}$ ratio for wildtype SecA and SecA-W701F, while this ratio changed sharply, but in opposite directions, for the two other mutant proteins. The $F_{330}/F_{355}$ ratio of SecA-W723F decreased during the endothermic transition, while that of wildtype SecA remained constant. Therefore, in the wildtype protein, the fluorescence of Trp723 must compensate for the observed relative decrease of $F_{330}/F_{355}$ in SecA-W723F (i.e., Trp723 is blue-shifted in wildtype SecA during the endothermic transition). For SecA-W775F, the $F_{330}/F_{355}$ increased during the endothermic transition, consistent with a red shift of Trp775 in wildtype SecA. In sum, it appears that Trp775 becomes more solvent exposed and Trp723 becomes more buried during the temperature-induced conformational change of SecA protein. These results are consistent with our quenching studies performed with LUV. They suggest that a similar conformational change takes place within the C-domain of SecA both during the endothermic transition in solution and when SecA interacts with model membranes.

*Effects of Signal Peptides on the Conformation of the C-Domain of SecA*. Recently, it has been established that signal peptides can specifically interact with SecA protein both in solution and in the presence of liposomes (*4*, *42*). To probe for signal peptide-induced conformational changes

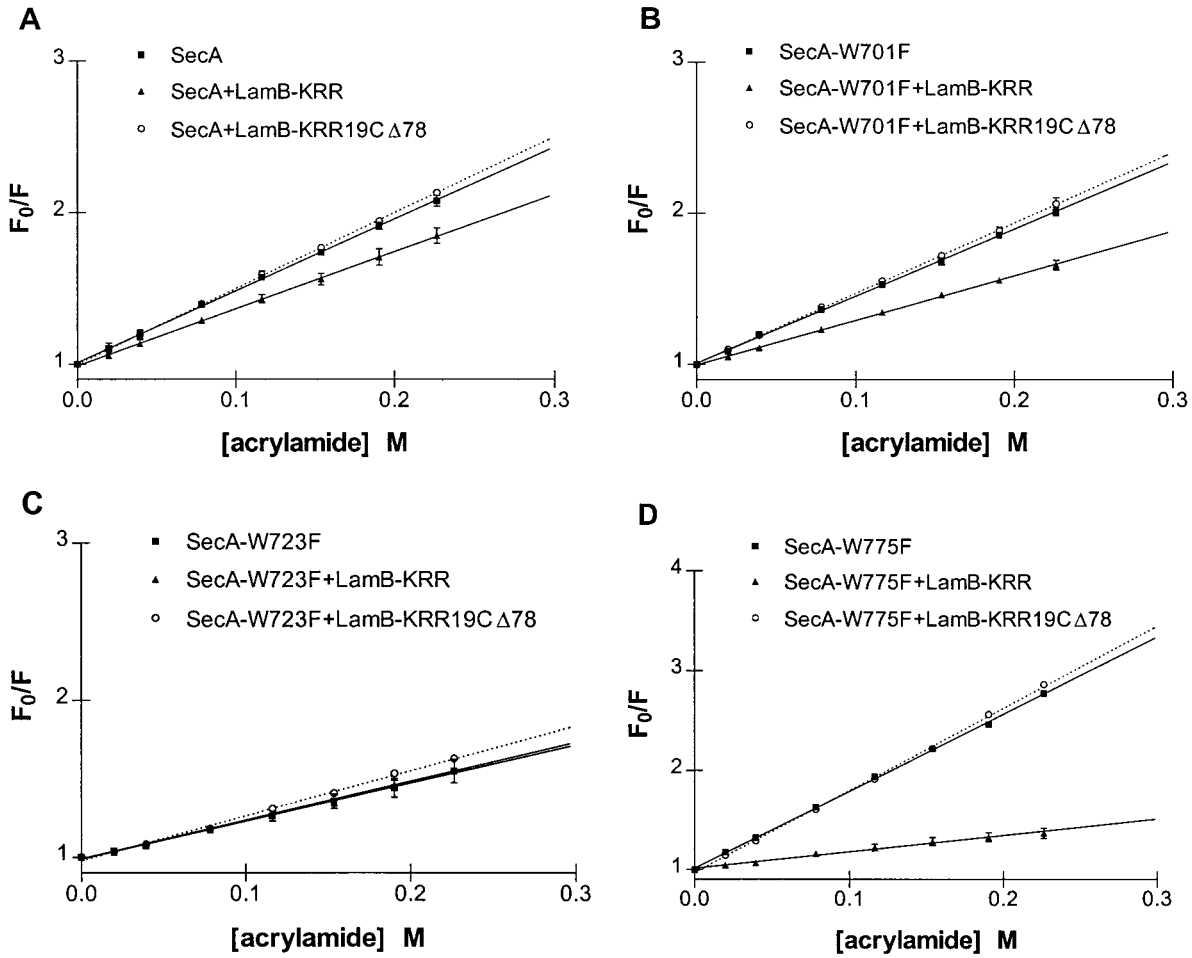


FIGURE 6: Stern−Volmer plots using acrylamide as the quencher for SecA proteins in the absence and presence of functional or nonfunctional signal peptide. (A) Wildtype SecA, (B) SecA-W701F, (C) SecA-W723F, and (D) SecA-W775F. SecA protein (0.1 $\mu$M) was incubated in the absence or presence of 2.0 $\mu$M LamB-KRR or LamB-KRR19CΔ78 in TKE buffer for 30 min prior to initiating the experiment. Fluorescence quenching experiments were conducted at 24 °C using 297 nm as the excitation wavelength and 340 nm as the emission wavelength. $F_0$ and $F$ are the fluorescence intensities in the absence and presence of acrylamide, respectively. Values were corrected for dilution.

of SecA, we studied the quenching of SecA fluorescence by acrylamide, utilizing LamB-KRR or LamB-KRR19CΔ78, functional or nonfunctional variants of the lambda receptor signal peptide, respectively. Figure 6 shows that the acrylamide quenching constant for SecA-W775F decreased markedly in the presence of functional signal peptide (79% decrease in $K_{SV}$, Table 1) as compared to no signal peptide or nonfunctional signal peptide. This result indicates an overall decrease in the solvent exposure of Trp701 and/or Trp723 in the presence of functional signal peptide. In contrast, a more modest effect was observed for wildtype SecA (27% decrease in $K_{SV}$, Table 1) or SecA-W701F (37% decrease in $K_{SV}$, Table 1), while little or no effect was observed for SecA-W723F. The modest decrease in $K_{SV}$ values observed for wildtype SecA and SecA-W701F suggest that Trp775 became more solvent exposed in the presence of functional signal peptide, thereby compensating in part for the decreased exposure of Trp701 and/or Trp723. This logic is consistent with the results observed for SecA-W723F, which showed no effect of signal peptide on its $K_{SV}$ value (presumably because of equal and opposite effects of Trp701 and Trp775). Furthermore, since SecA-W701F (containing Trp723 and Trp775) showed a modest signal peptide-dependent decrease in its $K_{SV}$ value, while SecA-W723F (containing Trp701 and Trp775) did not, it follows that Trp723 experienced a greater decrease in solvent exposure as compared to Trp701. Utilizing KI as a collisional quencher, Ahn and Kim (*42*) obtained a similar measurement for the signal peptide-dependent decrease in Trp solvent exposure for wildtype SecA protein. Finally, we note that exposure of SecA to signal peptide, LUV, or higher temperature all appear to change the local environments of Trp723 and Trp775. However, only Trp701 experienced a change in its local environment in the presence of signal peptide. The results of our quenching studies are summarized in Table 1.

## DISCUSSION

We initiated this study to elucidate further the conformational changes that occur when SecA interacts with its various ligands. Such conformational alterations serve to drive the protein translocation cycle, and their analysis should allow us to resolve the detailed steps that occur during this process. We approached this problem by creating a set of single Trp substitution variants of SecA protein and utilizing fluorescence spectroscopy to map out the environment of individual Trp residues of SecA and determine their response to important translocation ligands such as model membranes and signal peptide. This approach turned out to be a powerful one, since fortuitously the first four Trp residues of SecA

did not contribute significantly to the fluorescence spectrum in either of SecA's conformational states, allowing us to study the detailed behavior of the remaining three Trp residues within the C-domain of SecA. Our experience in this regard indicates the potential utility of a conservative mutagenic approach whereby individual or a limited number of Trp residues are altered within a large protein, thereby minimally perturbing its structural and biochemical properties.

Interpretation of our results relies on the structural and biochemical properties of our single Trp substitution mutant proteins being essentially normal. This point is supported by several observations: (i) the mutant proteins were active *in vivo* at wildtype SecA levels; (ii) they possessed normal endogenous, membrane, and translocation ATPase activities, a critical measure of SecA conformational cycling promoted by its translocation ligands; (iii) the phospholipid-binding activity of the mutant proteins was similar to wildtype SecA, and (iv) they displayed similar endothermic transition profiles as wildtype SecA protein. Taken together, these observations strongly suggest that this set of mutant proteins provides a valid basis for the study of SecA conformational dynamics and its modulation by translocation ligands.

The three Trp residues that we studied here, Trp701, Trp723, and Trp775 occupy distinct environments within SecA protein in its solution state. Both the position of peak Trp fluorescence as well as the acrylamide quenching data indicate that Trp723 and to a lesser extent Trp701 are relatively solvent accessible, while Trp775 appears to be buried within the interior of SecA protein. These results are consistent with those of den Blaauwen *et al*. (*23*), who studied the fluorescence properties of SecA proteins engineered to contain solely Trp701 or Trp775, as well as a recent model derived from the crystallization of *Bacillus subtilis* SecA protein (J. Hunt, S. Weinhauf, D. Oliver, and J. Deisenhofer, manuscript in preparation), which displays a 50% overall identity to its *E. coli* homologue (*33*, *43*). This model shows that the C-domain is composed of two helical subdomains, C1 and C2. The residue homologous to Trp775 (Trp724) is located in the middle of a helix that is shielded from solvent by two neighboring helices within C1, while Trp701 (Trp652) and Trp723 (Ile676) are located at the protein surface within a small bundle of helices that comprises C2.

Our results suggest that there is a similar change in the conformation of the C-domain of SecA in response to temperature or upon binding model membranes or signal peptide. Specifically it appears likely that during the endothermic transition or upon interaction with LUV or signal peptide, Trp775 became more solvent accessible, while Trp723 became less solvent exposed. In theory, while the observed changes in $K_{SV}$ value could be due to a change in either Trp exposure or excited state lifetime in the absence of quencher, an alteration in the latter parameter is much less common. In either case, our basic conclusion regarding the parallel conformational response of the C-domain to these conditions would be unaffected by this subtlety. Our result indicates that both C1 and C2 are affected by the conformational alteration that occurs in response to temperature or ligand binding. Of note, however, Trp701 did not respond in parallel to the different conditions, since its solvent accessibility changed only in the presence of signal peptide. This latter result is important, since it may provide a structural clue for positioning the signal peptide binding cleft or a signal peptide-specific conformational response or regulatory element within the C-domain of SecA protein. Additional studies are required to follow up on this potentially important observation.

Our results extend the initial observations by others in the field, who first noted that SecA conformation is sensitive to temperature or various translocation-related ligands. Specifically, they suggest that SecA alternates between more compact and extended states depending on its interaction with a particular ligand or the temperature of the system. ADP binding favors the more compact conformation of SecA, while binding to AMP−PNP, model membranes containing anionic phospholipids, signal peptide, preprotein, or increasing temperature all favor the more extended conformation of SecA (*4*, *6*, *15*, *23*, *40*, *42*). Since protease accessibility was often utilized to define these two states, it was unclear whether the extended conformation of SecA was the result of one or more distinct states, all of which were equally protease sensitive. In this regard, our study supports the existence of a single extended state of SecA, at least for the C-domain, since we obtained a similar pattern for the change in the local environments of Trp723 and Trp775 under these diverse conditions. Since we lacked environmental probes for other important regions of SecA, such as NBD-I, NBD-II, and the preprotein-binding region, additional studies will be needed to further resolve the effects that the different translocation ligands have on the conformation of other regions of SecA.

Both the N- and C-domains of SecA have been purported to undergo membrane cycling at SecYE in the presence of preprotein and ATP based on their alternating states of protease resistance (*7*, *8*). Evidence in favor of this model has also come from other groups, who showed that both the preprotein-binding region and the C-terminus of SecA were periplasmically exposed after SecA membrane insertion (*21*, *22*, *31*). These observations have left open precisely which regions of SecA interact with the various translocation ligands as well as the timing of the conformational response(s) and release of the ligands. Recently, we have shown that the N-domain of SecA contains the SecYE-binding determinant, while the C-domain binds phospholipids nonspecifically (*20*), consistent with a previous report that mapped a phospholipid binding determinant to the 70 C-terminal residues of SecA (*16*).

Taking our findings as well as those of other investigators into consideration, we suggest that the conformational flexibility of SecA is critical for driving the protein translocation cycle. For example, SecA proteins that confer azide resistant or signal sequence suppressor phenotypes had a lower endothermic transition temperature and a reduced affinity for ADP and a greatly accelerated ADP exchange rate (*24*), indicating the importance of N- and C-domain interaction and their flexibility for SecA function. A recent study found that SecA dimer is formed by association of N- and C-domains from adjacent protomers in an antiparallel fashion, and such association appears to regulate the SecA ATPase cycle (*44*). We propose that a tight association of the N- and C-domains is present in the compact state of SecA, while a looser association is found in the extended state of SecA. It seems likely that the conformational change

that we have followed here allows release of portions of the N- and C-domains of SecA for their penetration into the membrane, where portions of SecA and SecA-bound preprotein insert into the translocon. Presumably immediately prior to this event, SecA would have bound SecYE, preprotein, and ATP: ligands that serve to trigger this conformational transition. It is clear that SecA membrane cycling can also occur without SecA having bound all of the relevant translocation ligands, as occurs with default SecA membrane cycling that is promoted by AMP−PNP and does not require preprotein (*45*). The fact that both C1 and C2 are altered during the major conformational change of SecA suggests that it could be rather widespread, consistent with the need for at least some movement within the nucleotide- and preprotein-binding regions of SecA as well. Such issues can now be approached by the introduction of specific labels within these regions of SecA, and a similar methodology to that employed here can be utilized to address these and other related problems of interest.

## ACKNOWLEDGMENT

We thank Chris Damman for construction of the Trp substitution mutants and Lila Gierasch for the kind gift of the LamB signal peptides. This work was supported by Grant GM42033 from the National Institutes of Health to D.O. and the Patrick and Catherine Weldon Donaghue Medical Research Foundation (DF96-175) and the National Science Foundation (MCB-9507241) to I.M.

## REFERENCES

1. Danese, P. N., and Silhavy, T. J. (1998) *Annu. Rev. Genet. 32*, 59−94.
2. Fekkes, P., and Driessen, A. J. M. (1999) *Microbiol. Rev. 63*, 161−173.
3. Hartl, F.-U., Lecker, S., Schiebel, E., Hendrick, J. P., and Wickner, W. (1990) *Cell 63*, 269−279.
4. Wang, L., Miller, A., and Kendall, D. A. (2000) *J. Biol. Chem. 275*, 10154−10159.
5. Fekkes, P., de Wit, J. G., van der Wolk, J. P. W., Kimsey, H. H., Kumamoto, C. A., and Driessen, A. J. M. (1998) *Mol. Microbiol. 29*, 1179−1190.
6. Shinkai, A., Mei, L. H., Tokuda, H., and Mizushima, S. (1991) *J. Biol. Chem. 266*, 5827−5833.
7. Economou, A., and Wickner, W. (1994) *Cell 78*, 835−843.
8. Eichler, J., and Wickner, W. (1997) *Proc. Natl. Acad. Sci. U.S.A. 94*, 5574−5581.
9. van der Wolk, J. P. W., de Wit, J. G., and Driessen, A. J. M. (1997) *EMBO J. 16*, 7297−7304.
10. Nishiyama, K.-I., Suzuki, T., and Tokuda, H. (1996) *Cell 85*, 71−81.
11. Duong, F., and Wickner, W. (1997) *EMBO J. 16*, 4871−4879.
12. Mitchell, C., and Oliver, D. B. (1993) *Mol. Microbiol. 10*, 483−497.
13. Manting, E. H., van der Does, C., and Driessen, A. J. M. (1997) *J. Bacteriol. 179*, 5699−5704.
14. Mori, H., Sugiyama, H., Yamanaka, M., Sato, K., Tagaya, M., and Mizushima, S. (1998) *J. Biochem. 124*, 122−129.
15. Ulbrandt, N. D., London, E., and Oliver, D. B. (1992) *J. Biol. Chem. 267*, 15184−15192.
16. Breukink, E., Nouwen, N., van Raalte, A., Mizushima, S., Tommassen, J., and de Kruijff, B. (1995) *J. Biol. Chem. 270*, 7902−7907.
17. Kourtz, L., and Oliver, D. (2000) *Mol. Microbiol. 37*, 1342−1356.
18. Price, A., Economou, A., Duong, F., and Wickner, W. (1996) *J. Biol. Chem. 271*, 31580−31584.
19. Kimura, E., Akita, M., Matsuyama, S.-I., and Mizushima, S. (1991) *J. Biol. Chem. 266*, 6600−6606.
20. Dapic, V., and Oliver, D. (2000) *J. Biol. Chem. 275*, 25000−25007.
21. van der Does, C., den Blaauwen, T., de Wit, J. G., Manting, E., Groot, N., Fekkes, P., and Driessen, A. J. M. (1996) *Mol. Microbiol. 22*, 619−629.
22. Ramamurthy, V., and Oliver, D. (1997) *J. Biol. Chem. 272*, 23239−23246.
23. den Blaauwen, T., Fekkes, P., de Wit, J. G., Kuiper, W., and Driessen, A. J. M. (1996) *Biochemistry 35*, 11994−12004.
24. Schmidt, M., Ding, H., Ramamurthy, V., Mukerji, I., and Oliver, D. (2000) *J. Biol. Chem. 275*, 15440−15448.
25. Loewenthal, R., Sancho, J., and Fersht, A. R. (1991) *Biochemistry 30*, 6775−6779.
26. Chen, Y., and Barkley, M. D. (1998) *Biochemistry 37*, 9976−9983.
27. Clark, P. L., Weston, B. F., and Gierasch, L. M. (1998) *Curr. Biol. 3*, 401−412.
28. Tcherkasskaya, O., Ptitsyn, O. B., and Knutson, J. R. (2000) *Biochemistry 39*, 1879−1889.
29. McKnight, C. J., Rafalski, M., and Gierasch, L. M. (1991) *Biochemistry 30*, 9120−9127.
30. Lanzetta, P. A., Alvarez, L. J., Reinach, P. S., and Candia, O. A. (1979) *Anal. Biochem 100*, 95−97.
31. Kim, Y. J., Rajapandi, T., and Oliver, D. (1994) *Cell 78*, 845−853.
32. Cabelli, R. J. (1991) State University of New York, Stony Brook, NY.
33. Schmidt, M. G., Rollo, E. E., Grodberg, J., and Oliver, D. B. (1988) *J. Bacteriol. 170*, 3404−3414.
34. Lill, R., Cunningham, K., Brundage, L. A., Ito, K., Oliver, D., and Wickner, W. (1989) *EMBO J. 8*, 961−966.
35. Weber, G., and Shinitzky, M. (1970) *Proc. Natl. Acad. Sci. U.S.A. 65*, 823−830.
36. Eftink, M. (1991) in *Topics in Fluorescence Spectroscopy* (Lakowicz, J. R., Ed.) pp 53−126, Plenum Press, New York.
37. Song, M., and Hyoungman, K. (1997) *J. Biochem. 122*, 1010−1018.
38. Lill, R., Dowhan, W., and Wickner, W. (1990) *Cell 60*, 271−280.
39. Cabelli, R. J., Dolan, K. M., Qian, L., and Oliver, D. B. (1991) *J. Biol. Chem. 266*, 24420−24427.
40. Breukink, E., Demel, R. A., de Korte-Kool, G., and de Kruijff, B. (1992) *Biochem. 31*, 1119−1124.
41. Jiang, J. X., and London, E. (1990) *J. Biol. Chem. 265*, 8636−8641.
42. Ahn, T., and Hyoungman, K. (1996) *J. Biol. Chem. 271*, 12372−12379.
43. Sadaie, Y., Takamatsu, H., Nakamura, K., and Yamane, K. (1991) *Gene 98*, 101−105.
44. Karamanou, S., Vrontou, E., Slanidis, G., Baud, C., Roos, T., Kuhn, A., Politou, A. S., and Economou, A. (1999) *Mol. Microbiol. 35*, 1133−1145.
45. Economou, A., Pogliano, J. A., Beckwith, J., Oliver, D. B., and Wickner, W. (1995) *Cell 83*, 1171−1181.

BI002058W